Multilayered (Ti, Al) ceramic coating for high-speed machining applications

X. T. Zeng[a)]
Process Technology Division, Gintic Institute of Manufacturing Technology, 71 Nanyang Drive, Singapore 638075

Sam Zhang
School of Mechanical and Production Engineering, Nanyang Technological University, Singapore

L. S. Tan
Process Technology Division, Gintic Institute of Manufacturing Technology, 71 Nanyang Drive, Singapore 638075

(Received 7 September 2000; accepted 27 November 2000)

A multilayered (Ti, Al) ceramic hard coating was deposited on tunsten-carbide ball-nose end mills for high-speed machining using an unbalanced magnetron-sputtering system. The process parameter dependence of the coating properties was studied. X-ray diffractometry, x-ray photoelectron spectroscopy, nanoindentation, and scratch tests were used to characterize the structural, compositional, and mechanical properties of the coatings. High hardness, up to 40 GPa; good adhesion strength, up to 100 N in scratch critical load; and high-oxidation resistance were achieved, leading to excellent performance in high-speed milling on hardened tool steel at a speed of 260 $m\,min^{-1}$. The results show that the tool life with this coating is improved by a factor of 4 or better under the testing conditions used compared to the uncoated tools. The surface finish of the machined steel achieved with this coating is also significantly better. © *2001 American Vacuum Society.*
[DOI: 10.1116/1.1342868]

I. INTRODUCTION

With the demands of lower cost, higher accuracy, better surface finish, and shorter process time in the precision engineering industry, high-speed machining of high-hardness materials including hardened tool steels has become increasingly important. To improve the performance and to extend the life of the cutting tools, various types of hard coatings have been developed.

Hard coatings for high-speed machining consist of multiple layers because of the requirements for high-adhesion strength to the substrate, high-thermal stability, high-hardness, a low-friction coefficient, and good compatibility.[1–7] The present techniques used to produce these coatings include physical-vapor deposition, such as sputtering and ion plating, and plasma-enhanced chemical-vapor deposition.[8–9] Traditionally used coatings like TiN, CrN, and their alloyed nitride coatings, have high hardness and good adhesion strength on common materials used in the tooling industry. However, these coatings have poor performance in high-speed machining applications, especially in the cutting of hardened tool steels, because of phase transition (oxidation) at high temperatures. One of the most promising systems for this application is Ti–Al alloyed ceramic (nitride and/or carbide), which has high-thermal stability, a low-friction coefficient, and high hardness. Much work has been done worldwide to develop and commercialize this coating for high-speed cutting and milling tools.[1–4,8]

This article reports the development of a multilayered (Ti, Al) ceramic hard coating for high-speed machining tools using an unbalanced magnetron-sputtering system. The process parameter dependence of the coating properties was studied and discussed. High-speed-milling field testing on hardened tool steel was also investigated.

II. EXPERIMENTS

Coatings were deposited on WC substrates using a Teer 550 unbalanced magnetron-sputtering system.[5,6] Figure 1 shows a schematic diagram of the deposition chamber. Two pairs of rectangular Al and Ti targets were installed around a cylindrical vacuum chamber. High-purity argon and nitrogen were used as the discharge and reactive gases. The coating composition was controlled by the sputtering power applied

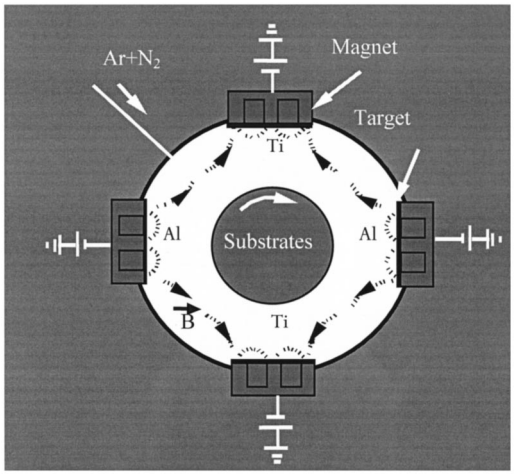

FIG. 1. Schematical diagram of the unbalanced magnetron-sputtering deposition system.

a)Author to whom correspondence should be addressed; electronic mail: xzeng@gintic.gov.sg

TABLE I. Basic deposition conditions for Al–Ti ceramic coatings.

Base pressure (Torr)	1.5×10^{-5}
Plasma cleaning	Biased at dc 980 V for 30 min
Deposition pressure (mTorr)	7–7.5
Power for Ti target	dc 2.8 kW
Power for Al target	1.2–2.1 kW
Substrate bias (V)	60–130
Substrate temperature (°C)	~300
N_2 partial pressure (mTorr)	0.5–1
Film thickness (μm)	2–3

to each target, and an optical emission monitor was used to monitor the poisoning status of the target surface. The basic deposition conditions are tabulated in Table I.

Figure 2 shows the coating design concept. The coating starts with a Ti bond layer, followed by a TiN interlayer, then gradually increases the Al content to form a graded Ti–Al–N transition layer, and finishes with an Al–Ti–N top layer. Ti has good bonding strength with WC and high-speed steel materials. This, together with the TiN transition layer, ensures good adhesion strength of the coating to the substrate. The top layer was processed as a multilayered structure to achieve both high hardness and low residual stress, and also high-oxidation resistance by alternatively depositing the Al-rich layer and Ti-rich layer, and also by using different plasma bombardments on the growing film surface.

The coating crystal structure was analyzed by x-ray diffractometry (XRD) using Cu $K\alpha$ x rays. The surface morphology and cross sections of the coatings were studied by scanning electron microscopy. For some samples, x-ray photoelectron spectroscopy (XPS) (VG Escalab 2201-XL) was used to measure the coating composition. To evaluate the microhardness and the adhesion strength, nanoindentation and scratch tests were carried out. Optical microscopy was used to confirm the starting point of the scratch failure.

For field testing of the coating performance, two fluted ϕ6 mm micrograin WC ball-nose end mills were selected as the test tools. The WC grain size is about 0.8 μm. A MIKRON HSM700 high-speed machining center was used for the milling experiments. The material used for the milling tests is

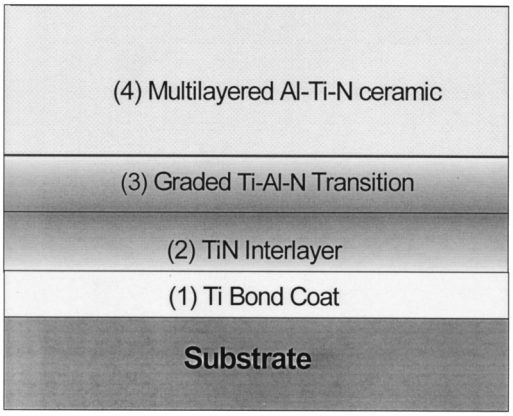

FIG. 2. Design concept of the Al–Ti–N coating. In layer (3), the relative content of Al:Ti was increased from 0 to 1:1.

TABLE II. Milling field test conditions and the properties of work material.

Cutting speed (m/min)	260
Depth of cut (mm)	0.2
Coolant	Air mist
Composition of the work material:	C: 0.38, Mn: 0.5, Cr: 13.6, V: 0.3
Hardened steel	Fe: balance
Rockwell hardness	HRC 52

AISI 420 tool steel hardened to HRC52. Table II tabulates the milling field test conditions and the main material properties. During the tests, the flank wear of the end mills was inspected and measured at an interval of every 5 m of machining using a Leica microscope with IMAGE database software. The magnification used was 50×. The maximum flank wear V_b' was recorded and analyzed. The tool life criterion is $V_b'=0.3$ mm. The total cutting distance before reaching this criterion was used to quantify the performance of the coating and the tool life of the tested end mill. At the end of each test, the milled surface roughness of the specimen was measured using a Taylor–Hobsons stylus profilometer.

III. RESULTS AND DISCUSSIONS

A. Structure and composition

Figure 3 shows a typical XRD spectrum of the AlTiN coating. The coating has a polycrystalline structure with (111) preferential growth. Depending on the substrate bias, the ratio of the relative intensity of the XRD peak (111) at $2\theta\sim37°$ to (200) at $2\ \theta\sim43°$ varied from 0.5 to 5, which strongly affects the mechanical properties of the coating (to be discussed later).

On the other hand, the composition and the relative content of Al to Ti are critical to the mechanical properties and oxidation resistance of the coatings, as evidenced by the adhesion, hardness, and oxidation temperature measurements. Stoichiometry or near stoichiometry is necessary to achieve high hardness and good adhesion strength. Increasing Al content can obviously increase the oxidation resistance, due to the formation of a dense Al_2O_3 layer on the surface of the coating. However, this reduces the hardness of the coating from 35–40 to 20–25 GPa. Another problem is that the Al-

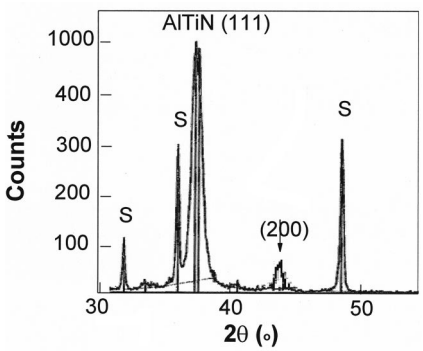

FIG. 3. XRD spectrum of AlTiN coating deposited under the substrate bias of 80 V. The peaks labeled with *s* are from the substrate diffraction.

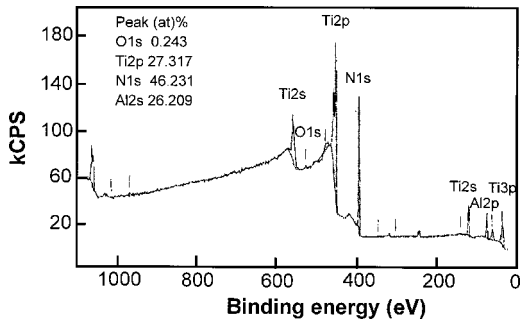

FIG. 4. XPS spectrum of AlTiN coating, obtained from the surface layer.

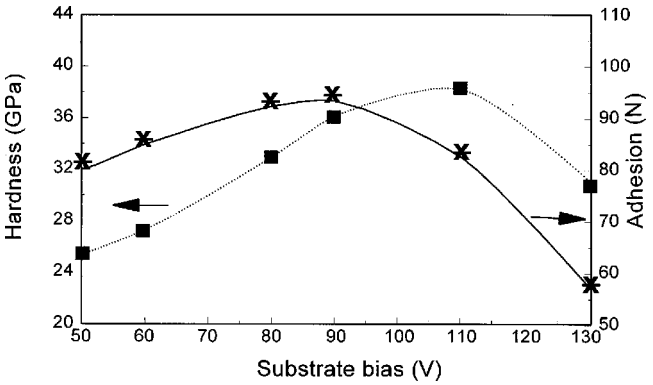

FIG. 6. Nanohardness and adhesion strength of AlTiN coatings as a function of substrate bias.

rich layer has low bonding strength with the base layer, regardless of whether it is pure metallic Ti, or ceramic TiN, resulting in poor adhesion of the coating. For this reason, a compositional grading process is necessary. Therefore, we deposited an Al–TiN transition layer on the TiN base layer, then a low-Al AlTiN support layer, followed by a high-Al top layer. The transition layer starts with an Al content of 0, and gradually increases to Al:Ti~1:1.5–2, the preset composition of the low-Al Al–Ti–N layer. The high-Al AlTiN layer has two designs, corresponding to two compositions: Al:Ti~1:1 and 2:1. The milling field tests show that the second design, i.e., Al:Ti~2:1, shows better performance, due to its better thermal stability. As an example, Fig. 4 shows the XPS spectrum obtained from the coating surface, and Fig. 5 shows the depth profiles of the atomic concentration in the top layer and the low-Al TiAlN sublayer. As designed, the top layer of the coating has a concentration of Al:Ti:N~1:1:1.8, a near-stoichiometric composition, and the sublayer has a concentration of Al:Ti:N~1:1.5:1.7. This combination provides the coating with good mechanical properties.

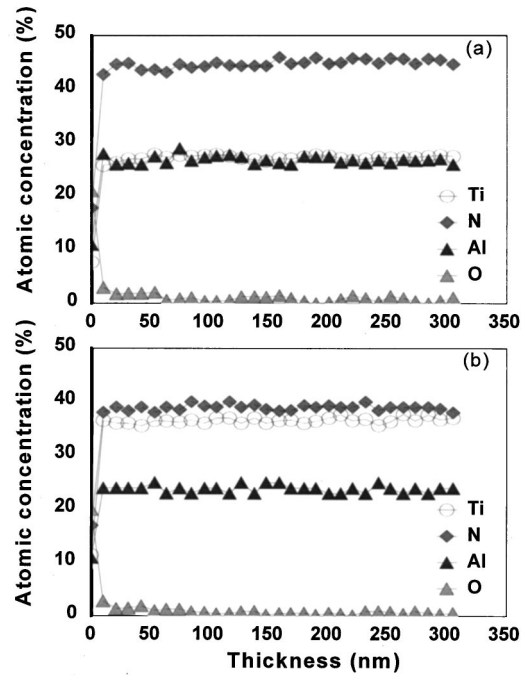

FIG. 5. Depth profiles of the atomic concentration in the (a) top layer and (b) low-Al AlTiN sublayer.

B. Hardness and adhesion

The main process parameters determining the mechanical properties of the coating include substrate bias power, sputtering power, and discharge and reactive gas flow rates.[10–13] Sputtering power and the reactive gas flow rates determine the composition of the coating. Provided the coating has a stoichiometric composition, the substrate bias, which provides effective ion bombardment on the substrate surface, is the most critical parameter to determine the crystalline structure, hardness, and adhesion. In this work, the dc bias from 50 to 130 V was tested. Figure 6 shows the bias dependence of the hardness and adhesion strength. Here, the nanohardness was calculated using the Oliver and Pharr method,[14] and the adhesion strength was represented by the critical load measured in the scratch test. With the increase of the bias power, the hardness increased substantially, and the adhesion strength first increased and then decreased in the range of 50–110 V, due to the increase in ion bombardment. Further increasing the bias power resulted in highly stressed films which cracked in some cases, and the adhesion strength substantially decreased. Therefore, reducing the internal stress without sacrificing the hardness is a key point to obtain good-quality coating.

C. High-speed-milling field testing

A total of nine cutters that are identical in geometry and tool material were field tested at a cutting speed of 260 m/min. Two of them were uncoated, two commercially TiAlN coated, and five graded AlTiN coated in this work. Setting the flank wear $V_b' = 0.3$ mm as the end-of-life indicator, the cutting distance of all nine testing end mills were recorded. The results are shown in Table III.

Apparently, all coated tools showed much improved tool life compared to the uncoated ones. All five cutters coated in this work have longer tool life when compared with the commercial ones. The best one, cutter No. 1, has a tool life of 93 m, which is about 4.7 times that of the uncoated end mill.

TABLE III. Milling field test results.

Cutters	Cutting distance (m)	Surface roughness (R_a, μm)
Uncoated Nos. 1 and 2	20	~0.4
Commercial TiAlN Coated Nos. 1 and 2	52	~0.4
Coated in this work:		
No. 1	93	0.26
Nos. 2 and 3	80	~0.32
Nos. 4 and 5	65	~0.38

Besides the good mechanical properties achieved in this coating, the unique thermal properties, which include oxidation resistance and heat insulation, play a critical role in this performance. Here, heat insulation or low thermal conductivity of AlTiN protects the cutting edge by insulating the tool substrate from damaging high temperatures and by dissipating the heat to the machining chips.

The surface finish of the work material is another important end-mill performance indicator. High smoothness, or low roughness is required in many applications such as mold and die machining. Also tabulated in Table III is the comparison of the surface roughness (R_a) achieved using the above end mills. Cutter No. 1 coated in this work shows the best surface finish with $R_a \sim 0.26$ μm, compared with 0.40 μm of the uncoated and commercial TiAlN-coated cutters. This surface finish satisfies the requirements for most applications in the precision machining industry.

IV. SUMMARY

A multilayered TiAlN coating was developed for high-speed machining tools. The coating shows good mechanical and thermal properties. High-speed-milling field testing shows that the tool life with these coatings is improved by a factor of 4 compared to the uncoated tools. The surface finish achieved with our coated tools is also significantly better.

ACKNOWLEDGMENTS

The authors would like to thank Dr. Fang Fengzhou, Dr. Alex Thoe, and Song Weijie for their technical assistance on high-speed-milling field tests.

[1]I. Dorfel, W. Osterle, I. Urban, and E. Bouzy, Surf. Coat. Technol. **111**, 199 (1999).
[2]A. Inspektor, C. E. Bauer, and E. J. Oles, Surf. Coat. Technol. **68/69**, 359 (1994).
[3]L. A. Donohue *et al.*, Surf. Coat. Technol. **93**, 69 (1997).
[4]M. Okumiya and M. Griepentrog, Surf. Coat. Technol. **112**, 123 (1999).
[5]X. T. Zeng, S. Zhang, and J. Hsieh, Surf. Coat. Technol. **102**, 108 (1998).
[6]X. T. Zeng, Surf. Coat. Technol. **113**, 75 (1999).
[7]X. T. Zeng, J. Vac. Sci. Technol. A **17**, 1991 (1999).
[8]C. W. Kim and K. H. Kim, Thin Solid Films **307**, 113 (1997).
[9]C. Pfohl, A. Gebauer-Teichmann, and K.-T. Rie, Surf. Coat. Technol. **112**, 347 (1999).
[10]A. A. Adjaottor *et al.*, Surf. Coat. Technol. **76-77**, 142 (1995).
[11]D. F. Lii, J. L. Huang, and M. H. Lin, Surf. Coat. Technol. **99**, 197 (1998).
[12]O. Knotek, F. Loffler, and L. Wolkers, Surf. Coat. Technol. **68/69**, 176 (1994).
[13]T. Leyendecker, O. Lemmer, S. Esser, and J. Ebberink, Surf. Coat. Technol. **48**, 175 (1991).
[14]W. C. Oliver and G. M. Pharr, J. Mater. Res. **7**, 1564 (1992).